Author/s:
Mobbs, JI;Black, KA;Tran, M;Burger, WAC;Venugopal, H;Holman, TR;Holinstat, M;Thal, DM;Glukhova, A

Title:
Cryo-EM structures of human arachidonate 12S-lipoxygenase bound to endogenous and exogenous inhibitors

Date:
2023-10-05

Citation:
Mobbs, J. I., Black, K. A., Tran, M., Burger, W. A. C., Venugopal, H., Holman, T. R., Holinstat, M., Thal, D. M. & Glukhova, A. (2023). Cryo-EM structures of human arachidonate 12S-lipoxygenase bound to endogenous and exogenous inhibitors. Blood, 142 (14), pp.1233-1242. https://doi.org/10.1182/blood.2023020441.

Persistent Link:
https://hdl.handle.net/11343/339118

blood®
Regular Article

PLATELETS AND THROMBOPOIESIS

Cryo-EM structures of human arachidonate 12S-lipoxygenase bound to endogenous and exogenous inhibitors

Jesse I. Mobbs,[1,2,*] Katrina A. Black,[3-5,*] Michelle Tran,[6] Wessel A. C. Burger,[2-5] Hariprasad Venugopal,[7] Theodore R. Holman,[6] Michael Holinstat,[8,9] David M. Thal,[1,2] and Alisa Glukhova[1-5]

[1]Drug Discovery Biology and [2]ARC Centre for Cryo-Electron Microscopy of Membrane Proteins, Monash Institute of Pharmaceutical Sciences, Monash University, Parkville, VIC, Australia; [3]Structural Biology Division, Walter and Eliza Hall Institute of Medical Research, Parkville, VIC, Australia; [4]Department of Medical Biology and [5]Department of Biochemistry and Pharmacology, University of Melbourne, Melbourne, VIC, Australia; [6]Department of Chemistry and Biochemistry, University of California, Santa Cruz, Santa Cruz, CA; [7]Ramaciotti Centre for Cryo-Electron Microscopy, Monash University, Clayton, VIC, Australia; and [8]Department of Pharmacology and [9]Department of Internal Medicine, Division of Cardiovascular Medicine, University of Michigan, Ann Arbor, MI

KEY POINTS

- **The first full-length structure of human arachidonate 12-LOX reveal mechanisms of its oligomeric and conformational states.**
- **The structures uncover the natural inhibitor of 12-LOX and reveal the binding site of inhibitor ML355.**

Human 12-lipoxygenase (12-LOX) is a key enzyme involved in platelet activation, and the regulation of its activity has been targeted for the treatment of heparin-induced thrombocytopenia. Despite the clinical importance of 12-LOX, the exact mechanisms by which it affects platelet activation are not fully understood, and the lack of structural information has limited drug discovery efforts. In this study, we used single-particle cryo-electron microscopy to determine high-resolution structures (1.7-2.8 Å) of human 12-LOX. Our results showed that 12-LOX can exist in multiple oligomeric states, from monomer to hexamer, which may affect its catalytic activity and membrane association. We also identified different conformations within the 12-LOX dimer, which likely represent different time points in its catalytic cycle. Furthermore, we identified small molecules bound to 12-LOX. The active site of the 12-LOX tetramer was occupied by an endogenous 12-LOX inhibitor, a long-chain acyl coenzyme A. In addition, we found that the 12-LOX hexamer can simultaneously bind to arachidonic acid and ML355, a selective 12-LOX inhibitor that has passed a phase 1 clinical trial for the treatment of heparin-induced thrombocytopenia and received a fast-track designation by the Food and Drug Administration. Overall, our findings provide novel insights into the assembly of 12-LOX oligomers, their catalytic mechanism, and small molecule binding, paving the way for further drug development targeting the 12-LOX enzyme.

Introduction

Platelet activation is essential for maintaining hemostasis. However, uncontrolled platelet activation leads to abnormal clot formation and an increased risk of thrombosis and cardiovascular disease.[1,2] Inhibition of platelet activation is an effective treatment that reduces the morbidity and mortality of cardiovascular ischemic events, such as myocardial infarction and stroke. Despite the use of antiplatelet therapies, such as aspirin and $P2Y_{12}$ receptor antagonists, to reduce thrombotic risk, a high prevalence of ischemic events leading to unacceptable levels of morbidity and mortality remains. Because of the continued risk of thrombosis, the development of alternative therapies to further limit occlusive thrombotic events is warranted.

The enzyme, human 12-lipoxygenase (12-LOX/ALOX12), is highly expressed in platelets,[3] and its activation leads to the production of 12-hydroperoxyeicosatetraenoic acid, a prothrombotic oxylipin.[4,5] Inhibition of 12-LOX prevents platelet activation,[6,7] has minimal effect on hemostasis, and does not promote increased bleeding, a common side effect of other antiplatelet therapies.[6,8,9] The selective 12-LOX inhibitor ML355[10] has passed phase 1 clinical trials for the treatment of heparin-induced thrombocytopenia and has received a fast-track designation by the Food and Drug Administration. Although 12-LOX is a promising target for antiplatelet therapies, there are no experimentally determined structures of human 12-LOX, thus limiting our understanding of the mechanism and regulation of 12-LOX activity. Although the structures of other LOX isozymes have been determined by X-ray

crystallography,[11-15] they do not provide enough information to fully comprehend the mechanism of 12-LOX oligomerization and inhibitor binding.

Here, we present the first high-resolution structures (range, 1.7-2.8 Å) of human 12-LOX determined using cryo-electron microscopy (cryo-EM). We show that 12-LOX possesses a protein fold similar to that of other lipoxygenases.[11-15] From a single sample of 12-LOX, we were able to determine the cryo-EM structures in multiple oligomeric forms, from the monomer to a hexamer. This observation is consistent with prior studies that have demonstrated the existence of multiple oligomeric forms of lipoxygenases, including monomers, dimers, and tetramers.[16-18] Similar to human 15-LOX, we also captured 12-LOX in different conformational states that likely reflect the different parts of the catalytic cycle for this enzyme: the open and closed conformations.[11] Because of the high-resolution features of the cryo-EM map, we were able to identify an endogenous 12-LOX inhibitor, a long-chain acyl coenzyme A (acyl-CoA), which co-purifies with the enzyme from mammalian cells. Finally, we were able to elucidate a putative allosteric binding site for the phase 2 inhibitor ML355. Collectively, we anticipate that these structures will guide further research on the function of 12-LOX in platelet activation and promote further drug discovery efforts for this clinically relevant enzyme.

Methods

A more detailed methods section is provided in the supplemental Data, which is available on the *Blood* website.

Expression and purification

Human 12-LOX was expressed in Expi293 cells. After cell lysis, the protein was purified using Nickel-affinity chromatography and size-exclusion chromatography (SEC).

Cryo-EM

Vitrification was performed at 1 mg/mL using UltrAufoil R1.2/1.3 300 mesh holey grids and Vitrobot Mark IV. Videos were collected at 0.82 Å per pixel on a G1 Titan Krios microscope with a K3 detector. Data processing was performed following standard pipelines in RELION version 3.1[19,20] and cryoSPARC[21] using MotionCor2[22] and GCTF.[23] The 3D variability analysis (3DVA)[24] was used to assess sample variability. Modeling was performed using AlphaFold Protein Structure Database,[25,26] ChimeraX,[27] Coot,[28] Phenix,[29] MolProbity,[30] and Grade web server.[31]

Steady-state kinetics and 50% inhibitory concentration determination

The 12-LOX enzyme kinetics was performed as described previously.[32]

Liposome binding

A lipid suspension was prepared with the following molar ratio: 99.9:0.1 1,2-dioleoyl-sn-glycero-3-phosphocholine (DOPC): 1,2-distearoyl-sn-glycero-3-phosphoethanolamine-N-[amino(polyethylene glycol)] (DSPE-PEG) (ie, DOPC). Liposomes were created according to a literature protocol[33] using a 100 nm filter at a final concentration of 10 mg/mL.

Results

High-resolution structures of 12S-lipoxygenase

Purification of 12-LOX from mammalian Expi293 cells yielded an oligomeric mixture of 12-LOX forms that were separated based on their size, using SEC (Figure 1; supplemental Figure 1). The 2 main peak fractions primarily corresponded to a dimer and a tetramer based on their size; however, the populations were heterogeneous and contained small amounts of other oligomeric forms (supplemental Figure 1E). Both SEC fractions displayed similar enzyme kinetics with a k_{cat} of 12 ± 0.9 s^{-1} for the dimer and 4.8 ± 0.2 s^{-1} for the tetramer. Both had a k_{cat}/K_M value of 1.4 ± 0.1 $s^{-1}\mu M^{-1}$. The enzyme activities of both SEC fractions were inhibited by ML355, with a 50% inhibitory concentration of 1.6 ± 0.3 μM and 1.4 ± 0.3 μM for the dimer and tetramer, respectively (supplemental Figure 1C-D; supplemental Table 2). Prior efforts to determine the structures of 12-LOX using X-ray crystallography likely failed because of the sample heterogeneity. Thus, we turned to cryo-EM to determine the structure of 12-LOX in each SEC fraction. To understand the binding mechanism of ML355, we added the inhibitor during protein expression and purification for the samples used in cryo-EM.

Unexpectedly, the dimer peak from the SEC 12-LOX purification gave rise to multiple high-resolution cryo-EM structures of 12-LOX in different oligomeric forms, including monomers (2.8 Å), dimers (2.5 Å), tetramers (2.3 Å), and hexamers (2.6 Å), all from the same imaged grid (Figure 1; supplemental Figures 2, 4, and 5; supplemental Table 1). In contrast, the tetramer peak yielded only a structure of the 12-LOX tetramer (Figure 1; supplemental Figures 3-5; supplemental Table 1) with an overall resolution of 1.8 Å. All oligomeric forms of 12-LOX exhibited significant intermolecular flexibility, as determined by the 3DVA in cryoSPARC (supplemental Videos 1-3).[24] Thus, we used local refinement (cryoSPARC) to improve the map resolution and quality of the individual subunits (supplemental Figures 2-5) within each oligomer. For the tetramer peak sample, this improved the resolution to 1.7 Å, allowing for accurate model building of full-length 12-LOX (residues G2-I663).

The structural architecture of 12-LOX is typical for lipoxygenases, with an N-terminal β-barrel polycystin-1-lipoxygenase α-toxin (PLAT) domain and C-terminal α-helical catalytic domain (Figure 2A). The structural alignment with other LOX structures (supplemental Figure 6A) revealed markedly similar folds, with root mean square deviations <1 Å, with the largest variations occurring in the PLAT domain (supplemental Figure 6B). The active site of 12-LOX is located in the catalytic domain, where the catalytic iron atom is coordinated by 3 conserved histidine residues (H360, H365, and H540) as well as N544 and the carboxyl (C) terminus of I663 (supplemental Figure 6C-D). Next to the catalytic iron was the typical LOX U-shaped lipid-binding pocket lined with hydrophobic residues. The entrance to the active site was bordered by an arched helix and the α2-helix in an extended conformation (Figure 2A; supplemental Figure 6C-D).

Oligomeric states of 12S-lipoxygenase

The biological unit of the 12-LOX oligomers appears to be a dimer arranged "head to toe." The tetramer and hexamer are made of a dimer of dimers and a trimer of dimers, respectively

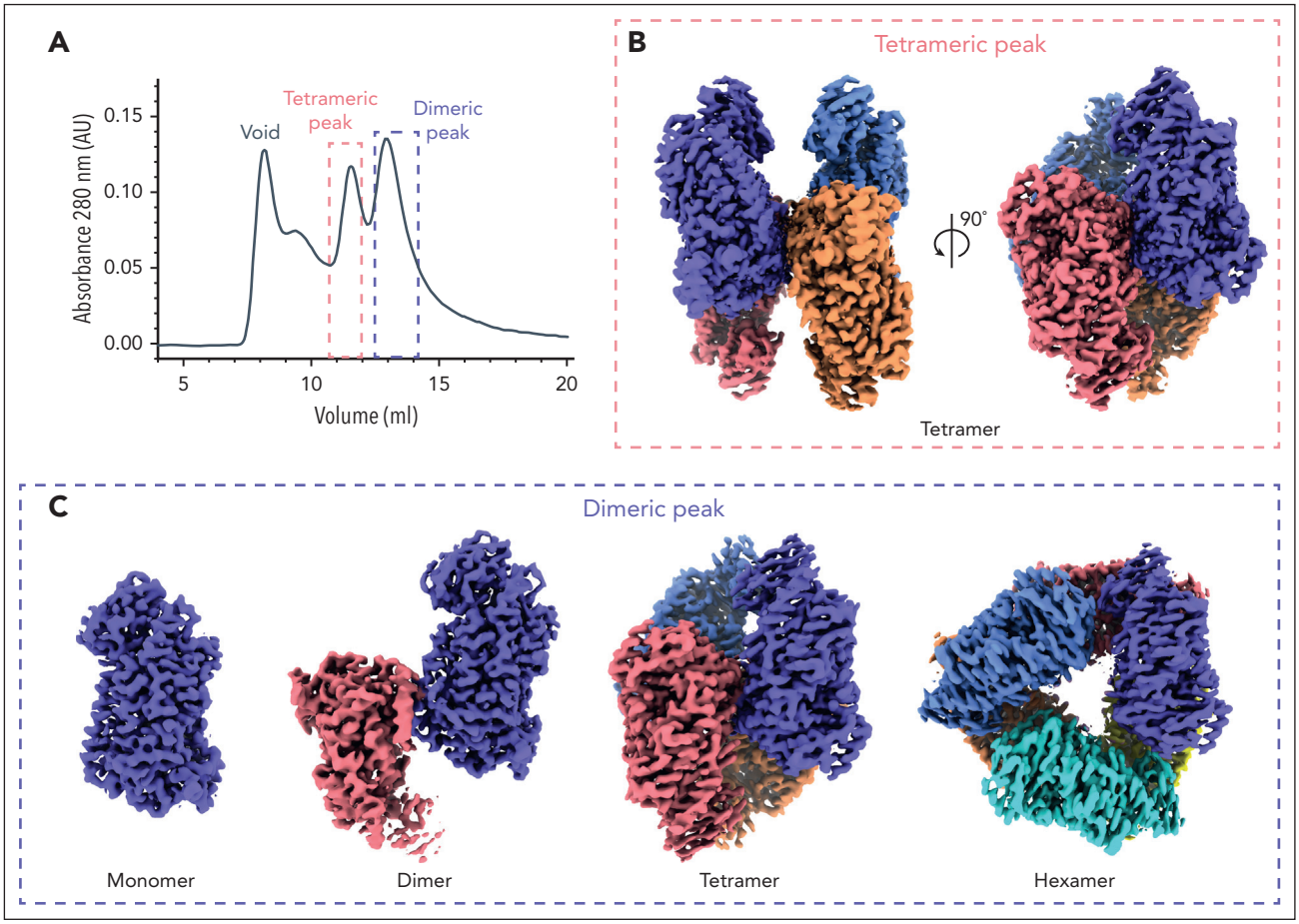

Figure 1. Different oligomeric forms of 12-LOX. (A) SEC UV absorbance trace (280 nm) of 12-LOX purification. 12-LOX separated as 2 distinct peaks, 1 corresponding to a tetramer (red box) and the other corresponding to a dimer (blue box). (B) Cryo-EM map of a 12-LOX tetramer from tetrameric SEC peak. (C) Cryo-EM maps of different 12-LOX oligomers resolved from dimeric SEC peak.

(Figures 1 and 2). The overall dimer substructure in each oligomeric form was maintained mainly through Van der Waals interactions between the α2-α4 helixes and the α3-α4 loop (Figure 2B-D). The dimer substructures of the 12-LOX tetramer and hexamer were virtually identical (root mean square deviations 0.78 Å), whereas the individual subunits of the dimer were rotated by 30° because of changes in the conformation of the α2-helix (described in "Conformational changes of 12S-lipoxygenase"; supplemental Figure 7). Higher-level oligomerization in 12-LOX tetramers was maintained through additional Van der Waals interactions of the α2-helix and hydrogen bond interactions of the arched helix and β9-β10 loop between neighboring subunits (Figure 2C). The architecture of the hexamers was supported by an additional hydrogen-bonding network and a disulfide bond (C89-C89) between the neighboring PLAT domains (Figure 2D).

Oligomerization of 12-LOX affects the accessibility of the active site to the bulk solvent. The entrance to the 12-LOX catalytic site is defined by the α2 and arched helices and is in the same plane as the predicted membrane-binding residues W70/L71/A180.[34] The entrance was accessible to the solvent in the 12-LOX monomer, dimer (the open subunit; described in "Conformational changes of 12S-lipoxygenase"), and hexamer but was obscured when the 2 dimers associated to form a tetramer because of the adjacent subunit. (supplemental Figure 8). Conversely, in the closed subunit of a 12-LOX dimer, occlusion was a result of a conformational change (explained in "Conformational changes of 12S-lipoxygenase").

To investigate whether oligomerization affects 12-LOX membrane binding, we tested the dimer and tetramer SEC fractions (Figure 1) for their ability to bind artificial DOPC liposomes. Both 12-LOX preparations bound liposomes to a similar extent (21% ± 6% and 36% ± 6% for dimers and tetramer peaks, respectively) (supplemental Figure 1B).

Conformational changes of 12S-lipoxygenase

The structure of the 12-LOX monomer in all oligomeric forms was similar, except for the 12-LOX dimer. Similar to the arrangement within the 12-LOX tetramer and hexamer, the monomers in the dimer were arranged "head-to-toe," with most of the contacts mediated via hydrophobic interactions between the α2-helixes (Figure 2B), as previously determined using hydrogen-deuterium exchange mass spectrometry (HDX-MS).[35] However, in contrast to the protein chains in the tetramer and hexamer, the individual subunits in the dimer were not equivalent. Instead, they adopted either an open conformation (as observed in the 12-LOX monomer, tetramer, and a hexamer) or a closed conformation, predominantly facilitated by a

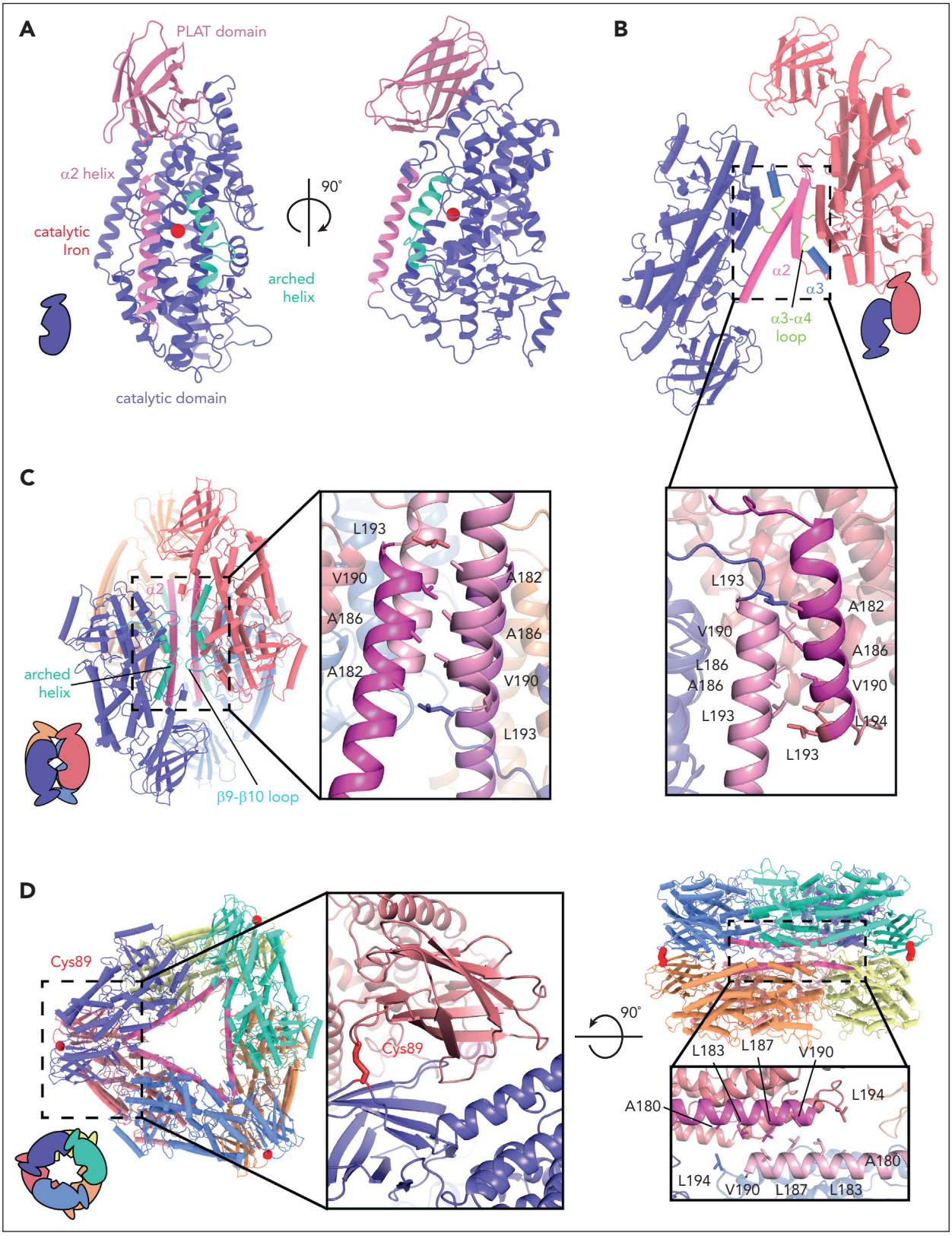

Figure 2. Oligomeric structures of 12-LOX. Models of 12-LOX as (A) monomer, (B) dimer, (C) tetramer, and (D) hexamer. Each subunit is represented by a different color and the α2-helix colored in pink and an arched helix in cyan. The graphical representation of each oligomeric state at the bottom left and inset details the oligomeric interface. Interacting amino acids are shown as sticks. (D) Cys89 (red) contributes a disulfide bridge to the interface of the hexamer. The Fe atom is shown as a red sphere.

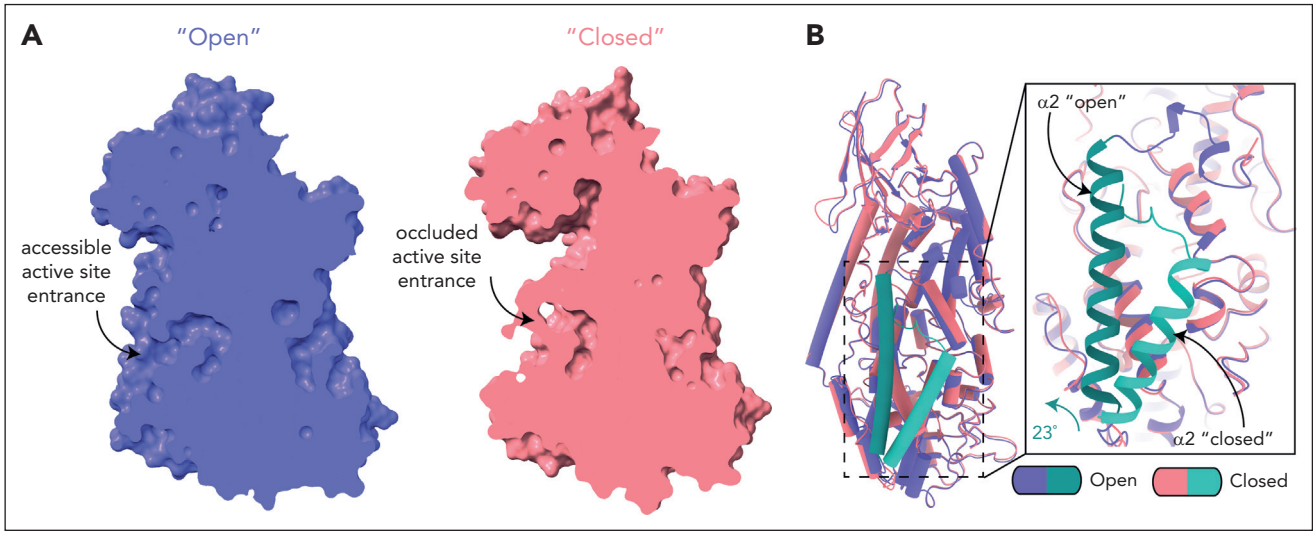

Figure 3. Conformational changes in the 12-LOX dimer. (A) Surface representation of 12-LOX in the open (left) and closed states (right), showing the active site cavity of the dimer 12-LOX subunits. In the open conformation, the cavity is occupied by a small molecule. (B) An alignment of open and closed states shows a 23° rotation and unwinding of the N-terminal residues of the α2-helix. The inset shows the zoomed-in view of the active site entrance. The α2-helix is in cyan.

large-scale motion of the α2-helix and corresponding rearrangements of the neighboring loops (Figure 3). In the open conformation, the α2-helix formed a long single helix at the edge of the active site. Conversely, in the closed conformation, the α2-helix underwent a rigid 23° pivot and rotation that blocked its entrance to the active site, reducing its internal volume (Figure 3B). The conformational change of the α2-helix also led to a 30° rotation of the 2 monomers relative to each other and to the dimer substructure observed in the 12-LOX tetramers and hexamers (supplemental Figure 7).

Natural inhibition of 12S-lipoxygenase by long-chain fatty acid acyl-CoAs

In all of our 12-LOX structures, the active site of the 12-LOX subunits in the open conformation was occupied by extra density in the cryo-EM maps (supplemental Figure 9), suggesting the presence of a bound ligand. The shape of the density varied between oligomeric forms, suggesting different ligands. The high-resolution of the tetramer (1.7 Å) and hexamer (2.3 Å) cryo-EM maps allowed us to model ligands into these densities confidently. However, because of the lower resolution of the monomer and dimer cryo-EM maps, we were unable to confidently identify bound molecules. We hypothesized that the observed densities were either ML355 or endogenous lipid(s) copurified from Expi293 cells.

The 12-LOX tetramer was made of a dimer of dimers with the lipid binding sites of the interdimer facing each other. The subunits at the interdimer interface face each other with their lipid binding sites (Figure 4A). Within each U-shaped pocket, we observed a density that resembled a lipid tail. Lipid density extended out of the binding site, spanning the gap between 2 neighboring subunits (supplemental Figure 10A). This density was also present in the apo 12-LOX tetramer samples that were expressed and purified in the absence of ML355, suggesting that the ligand was copurified from HEK293 cells (data not shown). To improve the resolution of the cryo-EM maps further, we performed 3DVA on individual subunits within a tetramer (supplemental Figure 10B; supplemental Video 2). Using the cluster mode of 3DVA, we were able to separate the protein chains that were fully occupied with the molecule and reconstructed the corresponding 12-LOX subunits and a full tetramer to a resolution of 1.9 and 2.05 Å, respectively (Figure 4A-C). Furthermore, 3DVA revealed that the lipid was bound only to 1 of the subunits at the interdimer interface at a time (thus, averaging to half lipid occupancy in the entire 12-LOX tetramer; supplemental Figure 10C; supplemental Video 4). In contrast, the opposite subunit was mostly empty, with some weak noncontinuous density in the active site, which could represent another unidentified lipid or incomplete separation of the occupied and unoccupied subunits during 3DVA.

Because of the high resolution and quality of the density map, we were able to identify the lipid as a fatty acid acyl-CoA ester, with a tail ~18 carbons long and of unknown saturation (oleoyl-CoA was used for modeling purposes; Figure 4B). The CoA headgroup was positioned at the interdimer interface at the entrance to the catalytic site, between the α2-helix and the arched helix, with the fatty acid tail extending into the U-shaped hydrophobic cavity (Figure 4C). The purine group of CoA formed CH-π interactions with I413, a hydrogen bond with Q406 of the arched helix, and cation-π interactions with R290 of the neighboring molecule (Figure 4D). The carbonyl group of oleic acid formed a hydrogen bond with H596. The 3 phosphate groups formed electrostatic interactions with R189, R290, and R585 of the bound 12-LOX as well as with R189, R290, K416, and R585 of the neighboring 12-LOX subunit. The overlay of these 2 subunits revealed that the polar residues at the dimeric interface underwent significant rearrangement to better accommodate the interaction with oleoyl-CoA (Figure 4F). The fatty acid tail extended into the catalytic site, forming extensive hydrophobic contacts (Figure 4E).

Because of the chemical lability of the thioester of acyl-CoA and the difficulty in detection by mass spectrometry, we set out to confirm our structural findings by determining whether fatty

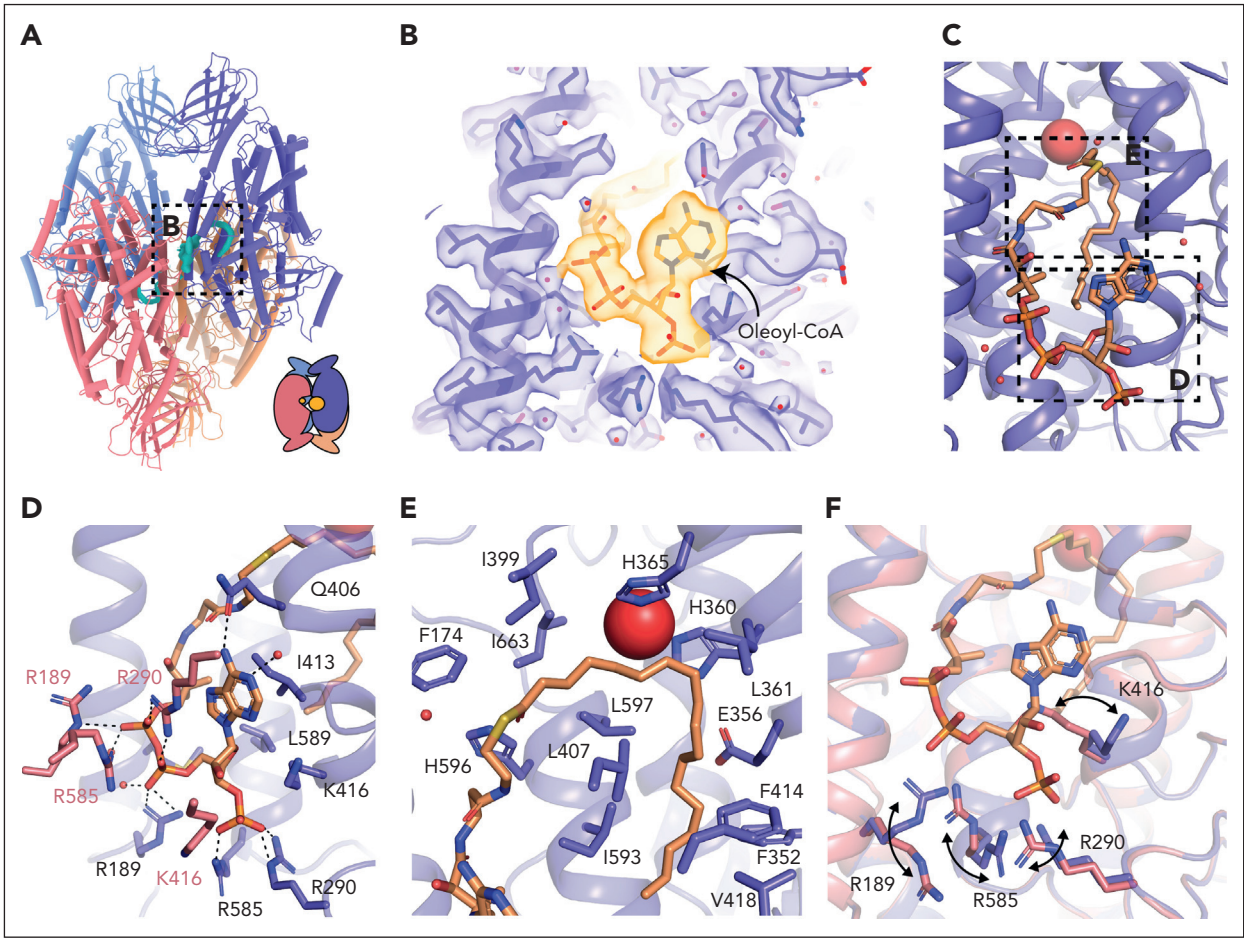

Figure 4. Acyl-CoA binding site in the 12-LOX tetramer. (A) Model of a 12-LOX tetramer, with density in the catalytic site shown in cyan. The graphical representation is shown in the right corner. (B) Acyl-CoA model and the density. Density is shown as a transparent surface, and the model as sticks colored by the heteroatoms. (C) Model of acyl-CoA within the catalytic site of 12-LOX. (D-E) 12-LOX residues in contact with acyl-CoA (orange) are shown as sticks. (D) Interactions of the adenosine triphosphate group. (E) Interactions of the acyl tail. (F) Conformational changes in the residues in contact with acyl-CoA. Acyl-CoA–bound subunit is shown in purple and unbound is shown in pink. Iron atom is shown as a red sphere.

acid acyl-CoAs inhibit 12-LOX. We tested a panel of long-chain acyl-CoAs with different lipid tail lengths and saturations to determine their ability to inhibit 12-LOX catalysis (supplemental Table 3). 12-LOX inhibition by acyl-CoAs depends on both their length and saturation status, with oleoyl-CoA (18:1) being the most potent inhibitor, with a 50% inhibitory concentration of 32 ± 4 μM. None of the tested acyl-CoAs were substrates for 12-LOX. These data confirmed that oleyl-CoA is the most potent inhibitor of 12-LOX, although the exact nature of the bound acyl-CoA in the structure is unconfirmed.

ML355 binding of 12-LOX

In contrast to the tetramer structure, the cryo-EM density within the active site of the 12-LOX hexamer was identical across subunits and distinct from that of acyl-CoA. Moreover, the density of the 2 independent molecules could be perfectly fit with arachidonic acid (AA) and ML355 (Figure 5). The AA molecule occupies the U-shaped hydrophobic cavity that was occupied by the fatty acid tail of acyl-CoA in the 12-LOX tetramer. The carboxyl group of AA interacts with 12-LOX via an H-bond with H596, as predicted,[36] positioning the C11-C12 double bond in the vicinity of the catalytic iron. The remainder of the contacts were from Van der Waals interactions with the hydrophobic residues lining the channel of the active site (Figure 5E). The position of AA was nearly identical to that of the anaerobic structure of coral 8R-LOX.[37]

Docking and mutagenesis studies predicted that ML355 binds deep in the 12-LOX active site,[32] but our cryo-EM density maps showed no evidence of ML355 occupying that region. Unexpectedly, however, a molecule of ML355 perfectly fit into the EM density found at the entrance to the active site in the hexamer. The interactions of ML355 with 12-LOX included the hydroxyl group of the 2-hydroxy-3-methoxyphenyl moiety, forming H-bonds with the backbone carbonyl of L178 and the amide of A182 (Figure 5D). The sulphur of the benzothiazole ring forms a H-bond with R189 while the sulphonyl group is within H-bonding distance to R290 and R585. The sulfonyl interactions of ML355 mimic the interactions observed with phosphates from oleoyl-CoA and residues R189, R290, and R585. The remaining molecule formed Van der Waals interactions with M185, I413, L589, and I593 (Figure 5D). To validate the ML355 binding pose, we generated 4 12-LOX mutants: L589A, L589F, 4A (R189A/R290A/R585A/K416A), and DLQN (R189D/R290L/K416Q/R585H) (Figure 5D). Although all mutants folded correctly (based on their thermal unfolding

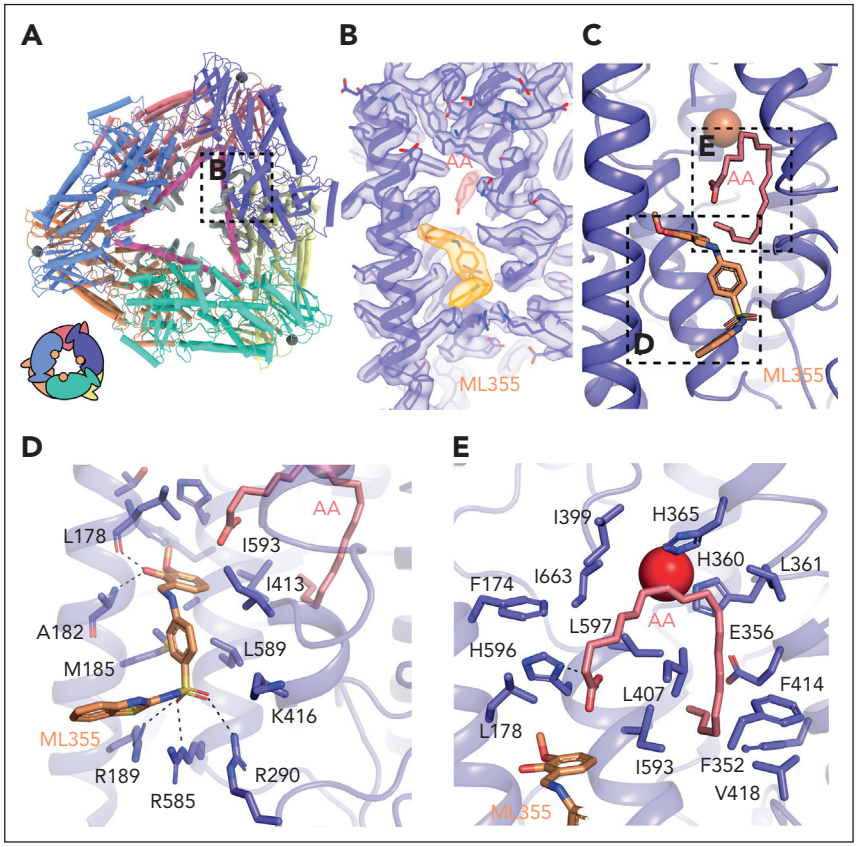

Figure 5. ML355 and AA binding sites in the 12-LOX hexamer. (A) Model of the 12-LOX hexamer with density at the catalytic site shown in gray. The graphical representation is shown in the bottom left corner. (B) Density of AA and ML355. Density is shown as a transparent surface, and the models as sticks (orange for ML355 and pink for AA) colored by heteroatoms. (C) Model of 12-LOX bound to ML355 and AA. (D-E) 12-LOX residues in contact with (D) ML355 (orange) and (E) AA (pink) are shown as sticks. Iron atom is shown as a red sphere.

profiles), L589F, 4A, and DLQN were catalytically inactive. Notably, the L589A mutation decoupled catalytic activity from ML355 inhibition (supplemental Figure 11A-B). This mutant displayed kinetics similar to that of wild-type 12-LOX but remained unresponsive to ML355 inhibition. Mass photometry demonstrated that L589A impaired the formation of higher-order oligomers associated with ML355 or acyl-CoA binding (supplemental Figure 11C). Although these results support the identified ML355 binding site, a more rigorous investigation of the mechanism of ML355 binding and inhibition is required in the future.

Discussion

To our knowledge, this is the first study to use cryo-EM to determine high-resolution structures of lipoxygenases. Compared with X-ray crystallography, the ability of cryo-EM to separate heterogeneous samples into discrete populations revealed distinct 12-LOX oligomeric states. Human LOXs display oligomeric diversity: although 5-LOX and 15-LOX primarily function as monomers, they dimerize at high protein and salt concentrations.[17] On the contrary, 12-LOX is primarily dimeric[38] but can form larger aggregates.[16] Other studies have suggested that most human LOXs form high-order oligomers in solution.[39] Our structures provide the first high-resolution insight into the diversity of 12-LOX oligomeric forms, which can likely be extended to other LOXs.

Small-angle X-ray scattering (SAXS) experiments predicted that all LOX dimers (12-LOX,[16] 15-LOX,[18] and 5-LOX[17]) have a similar organization, including the "head-to-toe" arrangement of individual monomers that interact through their α2-helixes. Before our structures, such an arrangement was only directly observed in the X-ray structures of rabbit 15-LOX-1[11,13] and human 15-LOX-2.[40] Although the overall dimer organization was similar among all 3 enzymes, the relative positions of the individual subunits varied owing to differences in specific interacting residues.

Cryo-EM allowed us, for the first time to our knowledge, to observe the structures of 12-LOX tetramers and hexamers. Interestingly, both are made from dimer building blocks that further oligomerize either into the dimer of dimers or trimer of dimers. Previous studies have suggested that reducing agents may prevent the oligomerization of 12-LOX,[16] suggesting that higher-order oligomers form through intramolecular disulfide bonds upon protein oxidation. Our 12-LOX hexamer structure is consistent with this observation because it is stabilized by an intermolecular disulfide bond (C89-C89). Other interactions in the dimer, tetramer, and hexamer included an extensive network of hydrophobic interactions and hydrogen bonds. As such, the assembly of 12-LOX into dimers and tetramers is independent of the oxidation state of the enzyme, whereas higher-molecular oligomers can represent a change in the oxidative environment of the cell.

Oligomerization of 12-LOX might be a regulatory mechanism for enzyme activity and/or membrane binding, because the accessibility of the active site varies between different oligomeric forms. The predicted membrane-binding residues for 12-LOX are located in the same plane as the entrance to its binding site

(supplemental Figure 8). Interestingly, the membrane-binding surface within the 12-LOX dimer building block (present in dimers, tetramers, and hexamers) is located within the same surface plane. However, in the tetramer and hexamer, the membrane-binding surface and active site entrance are further sequestered by interdimer contacts. As such, they may represent inactive states or storage pools for the enzyme. Although we did not observe significant differences in AA oxidation rates or DOPC liposome binding between the dimer and tetramer SEC peaks used for cryo-EM data collection, the data could possibly be explained by our heterogeneous preparations containing a mixture of 12-LOX oligomeric forms. Thus, further analysis using isolated 12-LOX oligomeric forms is necessary to better understand their roles in membrane binding and catalysis.

Intriguingly, higher-order oligomers of 15-LOX-1 were found to induce pore formation, leading to organelle clearance during erythrocyte maturation.[41] The 2-ring arrangement of the 12-LOX hexamer created a channel with a diameter of ~30 Å. Although the physiological role of this oligomeric species of 12-LOX requires further investigation, it is tempting to speculate that similar conformations might exist in other LOXs.

The protein chains in the 12-LOX monomer, tetramer, and hexamer adopt the open conformation characterized by an extended α2-helix that pack along the entrance to the active site. Such an α2 conformation is observed in many LOX structures, including coral 8R-LOX,[37] human 15-LOX-2,[14] and porcine 12-LOX (ALOX15).[15] In the 12-LOX dimer, 1 subunit adopts an open conformation, whereas the other undergoes a significant conformational change involving large-scale α2 movement. Alterations in the extended α2 conformation have been previously observed in the crystal structures of stable 5-LOX[12,42-44] (broken or disordered α2) and 15-LOX-1[11,13] (large-scale α2 movement). The 15-LOX-1 and, now, the 12-LOX are the only LOXs that were captured, forming nonsymmetrical dimers, with 1 subunit in the open and 1 in the closed conformations. Although the conformational change leading to the formation of the closed conformation differs in the degree of α2 movement and subunit rotation relative to each other, both result in the closure of the entrance to the active site.

The conformational change between the open and closed subunits in LOX dimers might be linked to their catalytic cycle[18] or be involved in inhibitor binding.[11] Similar to the 15-LOX-1 structure,[11] some of our 12-LOX oligomers demonstrated half the occupancy of their active sites. In the 12-LOX dimer, only the active site of the open subunit was occupied by what appears to be lipid density. This suggests that only half of the oligomeric subunits may be active at any given time, whereas the other subunit serves a regulatory role. This mechanism may be responsible for the differences in inhibitor binding observed previously between dimeric and monomeric 12-LOX (converted by introducing L183E/L187E mutations). Only the dimer showed inhibition by ML355 (K_i = 0.43 μM), whereas monomeric 12-LOX was unaffected.[35] Unfortunately, our dimer 12-LOX structure could not distinguish between part-of-the-site reactivity mechanisms, in which only 1 subunit is capable of catalysis, as described for cyclooxygenases,[45,46] and the flip-flop mechanism, in which catalysis alternates between subunits, as is the case for biotin carboxylase and transketolase.[47-49] Additional analysis is needed to further understand the 12-LOX catalytic mechanism.

One unexpected finding was the presence of the fatty acid acyl-CoA molecule in the 12-LOX tetramer that was copurified with our enzyme from Expi293 cells. Fatty acid acyl-CoA derivatives have long been known to inhibit platelet aggregation[50,51] in a chain-, length-, and saturation-dependent manner. Specifically, the medium-chain acyl-CoA (palmitoyl, stearoyl, oleoyl, and linoleoyl) inhibits lipoxygenase activity in platelets at concentrations ranging from 10 to 50 μM.[52] We confirmed that oleoyl-CoA inhibited 12-LOX at micromolar concentrations. Thus, the presence of acyl-CoA in the binding site is intriguing, particularly because the purified enzyme remained catalytically active. This paradox may be related to the 12-LOX reactivity mechanism and potential half-occupancy of the active sites (described earlier). However, the cause of half-site occupancy of the tetramer was different from that of the dimer, because the neighboring subunits create steric hindrance, preventing acyl-CoA binding to the opposing subunit. Considering that the levels of acyl-CoAs within the cell can reach micromolar concentrations,[53] long-chain acyl-CoAs could be physiologically important regulators of 12-LOX function in the cell. The effect of acyl-CoA on platelet aggregation is thought to be mediated by the P2Y1 and P2Y12 receptors.[54] However, with the discovery that fatty acid acyl-CoA directly binds and inhibits 12-LOX, it is possible that the inhibition of 12-LOX could also contribute to this process.

Despite the presence of ML355 during the expression and purification of 12-LOX, ML355 was only bound in the hexameric form of 12-LOX. It is likely that ML355 was competed out in the other oligomeric forms because of the presence of endogenous lipids. The observed pose of ML355 is in contradiction to previously published docking and mutagenesis studies that predicted ML355 binding deep in the 12-LOX active site.[32] However, the simultaneous binding of ML355 and AA observed in our structure could explain the mixed mode of ML355 inhibition, as described previously.[55] Nevertheless, future studies are needed to delineate the mechanism of ML355 inhibition with respect to different oligomeric forms of the enzyme, along with the role of endogenous inhibitors that may or may not be present in platelets.

In conclusion, this study presents the first high-resolution cryo-EM structure of 12-LOX in multiple oligomeric forms, provides the first structural information on the clinically relevant 12-LOX inhibitor ML355, shows evidence for conformational changes that might accompany the 12-LOX catalytic cycle, and demonstrates that acyl-CoA can serve as an endogenous 12-LOX inhibitor. This structural information will aid future studies on 12-LOX biology and its contribution to platelet activity, regulation of hemostasis, and thrombosis, and facilitate structure-based drug discovery efforts on a therapeutically validated enzyme for the regulation of immune thrombotic diseases such as heparin-induced thrombocytopenia and thrombosis.

Acknowledgments

The authors acknowledge the use of facilities within the Monash Ramaciotti Cryo-EM platform and the Ian Holmes Imaging Centre at the Bio21 Molecular Science and Biotechnology Institute. The computational work was supported by the MASSIVE high-performance data processing facility (MASSIVE HPC) (https://www.massive.org.au).

This work was supported by funding from the Walter and Eliza Hall Institute of Medical Research (WEHI), The University of Melbourne, and the estate of Akos and Marjorie Talon. A.G. is a CSL, Australia Centenary

Fellow. D.M.T. is supported by a National Health and Medical Research Council of Australia Early Career Investigator grant (1138448). M.H. is supported by National Institutes of Health, National Institute of General Medical Sciences grant R35 GM131835.

Authorship

Contribution: A.G. developed a protein purification strategy, performed protein expression, and negative stain transmission EM; A.G., and J.I.M. purified the protein; H.V. vitrified the sample and performed image acquisition at the Monash EM facility; J.I.M., K.A.B., and A.G. performed cloning, cryo-EM data processing, model building, refinement, and validation; M.T. performed enzyme kinetics, inhibition, and liposome binding; W.A.C.B. performed mass photometry and 12-LOX mutant purification, characterization, and kinetics; M.H. and T.R.H. participated in the experimental design and interpretation of results; A.G., D.M.T., J.I.M., and K.A.B. wrote the manuscript with contributions from all authors; and A.G. and D.M.T. supervised the project.

Conflict-of-interest disclosure: M.H. is an equity holder and serves on the scientific advisory board for Veralox Therapeutics and Cereno Scientific. M.H. and T.R.H. are coinventors of the patented compound ML355. The remaining authors declare no competing financial interests.

ORCID profiles: J.I.M., 0000-0001-6979-1427; K.A.B., 0000-0002-4094-6170; M.T., 0000-0002-7578-9347; W.A.C.B., 0000-0003-2047-2593; H.V., 0000-0001-5230-2973; T.R.H., 0000-0001-8072-2959; M.H., 0000-0001-5100-1933; D.M.T., 0000-0002-0325-2524; A.G., 0000-0003-4146-965X.

Correspondence: David M. Thal, Drug Discovery Biology, Monash Institute of Pharmaceutical Sciences, 399 Royal Parade, Parkville, VIC 3052, Australia; email: david.thal@monash.edu; and Alisa Glukhova, Structural Biology Division, WEHI, 1G Royal Parade, Parkville, VIC 3052, Australia; email: glukhova.a@wehi.edu.au.

Footnotes

Submitted 14 March 2023; accepted 19 July 2023; prepublished online on *Blood* First Edition 28 July 2023. https://doi.org/10.1182/blood.2023020441.

*J.I.M. and K.A.B. contributed equally to this study.

Atomic coordinates and the cryo-EM density maps have been deposited in the Protein Data Bank and the Electron Microscopy Data Bank (accession codes 8GHB and EMD-40039 for 12-LOX monomers; 8GHC and EMD-40040, EMD-40299, EMD-4030, EMD-40300 for dimers; 8GHE and EMD-40042 for tetramers and 8GHD and EMD-4004, EMD-40302, EMD-40304 for hexamers).

Data are available on request from the corresponding authors, David M. Thal (david.thal@monash.edu) and Alisa Glukhova (glukhova.a@wehi.edu.au).

The online version of this article contains a data supplement.

There is a *Blood* Commentary on this article in this issue.

The publication costs of this article were defrayed in part by page charge payment. Therefore, and solely to indicate this fact, this article is hereby marked "advertisement" in accordance with 18 USC section 1734.

REFERENCES

1. Lebas H, Yahiaoui K, Martos R, Boulaftali Y. Platelets are at the nexus of vascular diseases. *Front Cardiovasc Med*. 2019;6:132.
2. Willoughby S, Holmes A, Loscalzo J. Platelets and cardiovascular disease. *Eur J Cardiovasc Nurs*. 2002;1(4):273-288.
3. Burkhart JM, Vaudel M, Gambaryan S, et al. The first comprehensive and quantitative analysis of human platelet protein composition allows the comparative analysis of structural and functional pathways. *Blood*. 2012;120(15):e73-82.
4. Hamberg M, Samuelsson B. Prostaglandin endoperoxides. Novel transformations of arachidonic acid in human platelets. *Proc Natl Acad Sci U S A*. 1974;71(9):3400-3404.
5. Ikei KN, Yeung J, Apopa PL, et al. Investigations of human platelet-type 12-lipoxygenase: role of lipoxygenase products in platelet activation. *J Lipid Res*. 2012;53(12):2546-2559.
6. Adili R, Tourdot BE, Mast K, et al. First selective 12-LOX inhibitor, ML355, impairs thrombus formation and vessel occlusion in vivo with minimal effects on hemostasis. *Arterioscler Thromb Vasc Biol*. 2017;37(10):1828-1839.
7. Yeung J, Tourdot BE, Fernandez-Perez P, et al. Platelet 12-LOX is essential for FcgammaRIIa-mediated platelet activation. *Blood*. 2014;124(14):2271-2279.
8. Svensson Holm AC, Grenegard M, Ollinger K, Lindstrom EG. Inhibition of 12-lipoxygenase reduces platelet activation and prevents their mitogenic function. *Platelets*. 2014;25(2):111-117.
9. Yeung J, Li W, Holinstat M. Platelet signaling and disease: targeted therapy for thrombosis and other related diseases. *Pharmacol Rev*. 2018;70(3):526-548.
10. Luci D, Jameson JB, Yasgar A, et al. Discovery of ML355, a potent and selective inhibitor of human 12-lipoxygenase. In: *Probe Reports from the NIH Molecular Libraries Program [Internet]*. Bethesda (MD): National Center for Biotechnology Information (US); 2013:2010.
11. Choi J, Chon JK, Kim S, Shin W. Conformational flexibility in mammalian 15S-lipoxygenase: reinterpretation of the crystallographic data. *Proteins*. 2008;70(3):1023-1032.
12. Gilbert NC, Bartlett SG, Waight MT, et al. The structure of human 5-lipoxygenase. *Science*. 2011;331(6014):217-219.
13. Gillmor SA, Villasenor A, Fletterick R, Sigal E, Browner MF. The structure of mammalian 15-lipoxygenase reveals similarity to the lipases and the determinants of substrate specificity. *Nat Struct Biol*. 1997;4(12):1003-1009.
14. Kobe MJ, Neau DB, Mitchell CE, Bartlett SG, Newcomer ME. The structure of human 15-lipoxygenase-2 with a substrate mimic. *J Biol Chem*. 2014;289(12):8562-8569.
15. Xu S, Mueser TC, Marnett LJ, Funk MO Jr. Crystal structure of 12-lipoxygenase catalytic-domain-inhibitor complex identifies a substrate-binding channel for catalysis. *Structure*. 2012;20(9):1490-1497.
16. Aleem AM, Jankun J, Dignam JD, et al. Human platelet 12-lipoxygenase, new findings about its activity, membrane binding and low-resolution structure. *J Mol Biol*. 2008;376(1):193-209.
17. Hafner AK, Cernescu M, Hofmann B, et al. Dimerization of human 5-lipoxygenase. *Biol Chem*. 2011;392(12):1097-1111.
18. Ivanov I, Shang W, Toledo L, et al. Ligand-induced formation of transient dimers of mammalian 12/15-lipoxygenase: a key to allosteric behavior of this class of enzymes? *Proteins*. 2012;80(3):703-712.
19. Zivanov J, Nakane T, Forsberg BO, et al. New tools for automated high-resolution cryo-EM structure determination in RELION-3. *Elife*. 2018;7:e42166.
20. Scheres SHW. A Bayesian view on cryo-EM structure determination. *J Mol Biol*. 2012;415(2):406-418.
21. Punjani A, Rubinstein JL, Fleet DJ, Brubaker MA. cryoSPARC: algorithms for rapid unsupervised cryo-EM structure determination. *Nat Methods*. 2017;14(3):290-296.
22. Zheng SQ, Palovcak E, Armache J-P, Verba KA, Cheng Y, Agard DA. MotionCor2: anisotropic correction of beam-induced motion for improved cryo-electron microscopy. *Nat Methods*. 2017;14(4):331-332.

23. Zhang K. Gctf: real-time CTF determination and correction. *J Struct Biol*. 2016;193(1):1-12.

24. Punjani A, Fleet DJ. 3D variability analysis: resolving continuous flexibility and discrete heterogeneity from single particle cryo-EM. *J Struct Biol*. 2021;213(2):107702.

25. Varadi M, Anyango S, Deshpande M, et al. AlphaFold Protein Structure Database: massively expanding the structural coverage of protein-sequence space with high-accuracy models. *Nucleic Acids Res*. 2022;50(D1):D439-D444.

26. Jumper J, Evans R, Pritzel A, et al. Highly accurate protein structure prediction with AlphaFold. *Nature*. 2021;596(7873):583-589.

27. Pettersen EF, Goddard TD, Huang CC, et al. UCSF ChimeraX: structure visualization for researchers, educators, and developers. *Protein Sci*. 2021;30(1):70-82.

28. Emsley P, Lohkamp B, Scott WG, Cowtan K. Features and development of Coot. *Acta Crystallogr D*. 2010;66(pt 4):486-501.

29. Adams PD, Afonine PV, Bunkóczi G, et al. PHENIX: a comprehensive Python-based system for macromolecular structure solution. *Acta Crystallogr D*. 2010;66(pt 2):213-221.

30. Chen VB, Arendall WB 3rd, Headd JJ, et al. MolProbity: all-atom structure validation for macromolecular crystallography. *Acta Crystallogr D Biol Crystallogr*. 2010;66(pt 1):12-21.

31. Smart OS, Womack TO, Sharff A, et al. Grade v.1.2.13. *Global Phasing*. 2011. Accessed 18 October 2022. www.globalphasing.com

32. Tsai WC, Aleem AM, Tena J, et al. Docking and mutagenesis studies lead to improved inhibitor development of ML355 for human platelet 12-lipoxygenase. *Bioorg Med Chem*. 2021;46:116347.

33. Voss OH, Lee HN, Tian L, Krzewski K, Coligan JE. Liposome preparation for the analysis of lipid-receptor interaction and efferocytosis. *Curr Protoc Immunol*. 2018;120:14.44.1-14.44.21.

34. Walther M, Anton M, Wiedmann M, Fletterick R, Kuhn H. The N-terminal domain of the reticulocyte-type 15-lipoxygenase is not essential for enzymatic activity but contains determinants for membrane binding. *J Biol Chem*. 2002;277(30):27360-27366.

35. Tsai WC, Aleem AM, Whittington C, et al. Mutagenesis, hydrogen-deuterium exchange, and molecular docking investigations establish the dimeric interface of human platelet-type 12-lipoxygenase. *Biochemistry*. 2021;60(10):802-812.

36. Aleem AM, Tsai WC, Tena J, et al. Probing the electrostatic and steric requirements for substrate binding in human platelet-type 12-lipoxygenase. *Biochemistry*. 2019;58(6):848-857.

37. Neau DB, Bender G, Boeglin WE, Bartlett SG, Brash AR, Newcomer ME. Crystal structure of a lipoxygenase in complex with substrate. *J Biol Chem*. 2014;289(46):31905-31913.

38. Shang W, Ivanov I, Svergun DI, et al. Probing dimerization and structural flexibility of mammalian lipoxygenases by small-angle X-ray scattering. *J Mol Biol*. 2011;409(4):654-668.

39. Aleem AM, Wells L, Jankun J, et al. Human platelet 12-lipoxygenase: naturally occurring Q261/R261 variants and N544L mutant show altered activity but unaffected substrate binding and membrane association behavior. *Int J Mol Med*. 2009;24(6):759-764.

40. Tsai WC, Gilbert NC, Ohler A, et al. Kinetic and structural investigations of novel inhibitors of human epithelial 15-lipoxygenase-2. *Bioorg Med Chem*. 2021;46:116349.

41. van Leyen K, Duvoisin RM, Engelhardt H, Wiedmann M. A function for lipoxygenase in programmed organelle degradation. *Nature*. 1998;395(6700):392-395.

42. Gallegos EM, Reed TD, Mathes FA, et al. Helical remodeling augments 5-lipoxygenase activity in the synthesis of proinflammatory mediators. *J Biol Chem*. 2022;298(9):102282.

43. Gilbert NC, Gerstmeier J, Schexnaydre EE, et al. Structural and mechanistic insights into 5-lipoxygenase inhibition by natural products. *Nat Chem Biol*. 2020;16(7):783-790.

44. Gilbert NC, Rui Z, Neau DB, et al. Conversion of human 5-lipoxygenase to a 15-lipoxygenase by a point mutation to mimic phosphorylation at Serine-663. *FASEB J*. 2012;26(8):3222-3229.

45. Yuan C, Rieke CJ, Rimon G, Wingerd BA, Smith WL. Partnering between monomers of cyclooxygenase-2 homodimers. *Proc Natl Acad Sci U S A*. 2006;103(16):6142-6147.

46. Yuan C, Sidhu RS, Kuklev DV, et al. Cyclooxygenase allosterism, fatty acid-mediated cross-talk between monomers of cyclooxygenase homodimers. *J Biol Chem*. 2009;284(15):10046-10055.

47. Sevostyanova I, Solovjeva O, Selivanov V, Kochetov G. Half-of-the-sites reactivity of transketolase from Saccharomyces cerevisiae. *Biochem Biophys Res Commun*. 2009;379(4):851-854.

48. Janiyani K, Bordelon T, Waldrop GL, Cronan JE Jr. Function of Escherichia coli biotin carboxylase requires catalytic activity of both subunits of the homodimer. *J Biol Chem*. 2001;276(32):29864-29870.

49. Wielgus-Kutrowska B, Grycuk T, Bzowska A. Part-of-the-sites binding and reactivity in the homooligomeric enzymes - facts and artifacts. *Arch Biochem Biophys*. 2018;642:31-45.

50. Lin C, Lubin B, Smith S. Inhibition of platelet aggregation by acyl-CoA thioesters. *Biochim Biophys Acta*. 1976;428(1):45-55.

51. Lascu I, Edwards B, Cucuianu MP, Deamer DW. Platelet aggregation is inhibited by long chain acyl-CoA. *Biochem Biophys Res Commun*. 1988;156(2):1020-1025.

52. Fujimoto Y, Tsunomori M, Sumiya T, Nishida H, Sakuma S, Fujita T. Effects of fatty acyl coenzyme a esters on lipoxygenase and cyclooxygenase metabolism of arachidonic acid in rabbit platelets. *Prostaglandins Leukot Essent Fatty Acids*. 1995;52(4):255-258.

53. Abranko L, Williamson G, Gardner S, Kerimi A. Comprehensive quantitative analysis of fatty-acyl-coenzyme A species in biological samples by ultra-high performance liquid chromatography-tandem mass spectrometry harmonizing hydrophilic interaction and reversed phase chromatography. *J Chromatogr A*. 2018;1534:111-122.

54. Manolopoulos P, Glenn JR, Fox SC, et al. Acyl derivatives of coenzyme A inhibit platelet function via antagonism at P2Y1 and P2Y12 receptors: a new finding that may influence the design of anti-thrombotic agents. *Platelets*. 2008;19(2):134-145.

55. Luci DK, Jameson JB 2nd, Yasgar A, et al. Synthesis and structure-activity relationship studies of 4-((2-hydroxy-3-methoxybenzyl) amino)benzenesulfonamide derivatives as potent and selective inhibitors of 12-lipoxygenase. *J Med Chem*. 2014;57(2):495-506.